JOURNAL OF MATERIALS SCIENCE 35 (2000) 5157–5168

Lamellar thickening growth of an extended chain single crystal of polyethylene (II): ΔT dependence of lamellar thickening growth rate and comparison with lamellar thickening

M. HIKOSAKA, K. AMANO
Faculty of Integrated Arts and Sciences, Hiroshima University, Higashi-Hiroshima, 739-8521 Japan
E-mail: hikosaka @hiroshima-u.ac.jp

S. RASTOGI
Laboratory of Polymer Chemistry and Technology, Technische Universiteit Eindhoven, Eindhoven, The Netherlands

A. KELLER
H. H. Wills Physics Laboratory, University of Bristol, Bristol, BS8 1TL, UK

The degree of supercooling (ΔT^0) dependence of lamellar thickening growth rate (U) of an isolated extended chain single crystal (ECSC) of polyethylene is studied. The experimental formula, $U = C\exp(-D/\Delta T^0)$, where $C = 130$ nm/s and $D = 20.0$ K is obtained for the first time. The formula is the same as that of lateral growth rate (V). The reason why U and V obey the same formula is well explained by a model named "sliding diffusion model of the lamellar thickening growth". The model proposed that the lamellar thickening growth is controlled by both chain sliding diffusion within the ECSC and the nucleation on the side surface. The observed fact that the U increases with increase of ΔT^0 is opposite to the well known fact that lamellar thickening rate W decreases with increase of ΔT^0. This siginificant difference was well explained by the difference between the "primary crystallization" and the "secondary crystallization", which is a kind of "Ostwald's ripening process". The origin of the "tapered shape" is well explained by coupling of lamellar thickening and lateral growths. © *2000 Kluwer Academic Publishers*

1. Introduction

In the previous paper which is named Part I [1] of the series of the "Thickening growth papers", we have shown that an isolated extended chain single crystal (ECSC) of polyethylene (PE) is formed through two different growth mechanisms, namely newly found lamellar thickening growth and well known lateral growth mechanisms [2, 3]. A crystal grows in two different directions simultaneously; one is parallel and the other is perpendicular to the chain axis, which correspond to the lamellar thickening growth and the lateral growth, respectively. We showed in the Part I paper that the tapered shape seen on the cross section of an isolated ECSC is a characteristic shape of a polymer single crystal and that the tapered shape is evidence for the lamellar thickening growth. It is shown that the lamellar thickening growth rate (U) is obtained from the combination of the mapping of the tapered shape and the lateral growth rate (V), which we named the "mapping method" [1–3].

In the "mapping method", the lamellar thickness of an ECSC (l) is observed (="mapped") as a function of lateral distance (x) counted from the tip of the ECSC. The x can be transformed to time t by applying the relation, $x = Vt$, which is a definition of V. Thus the U can be obtained using a relation, $U = (\mathrm{d}l/\mathrm{d}t)/2$, which is definition of U.

It is well known that crystallization is driven by the free energy difference between isotropic and crystalline phases. The driving force in the melt crystallization is the free energy of fusion (Δg) which is in proportion to the degree of supercooling (ΔT^0), i.e., $\Delta g \propto \Delta T^0$. Therefore it is important to obtain the ΔT dependence of the growth rates in order to make clear the molecular mechanism of the growth.

We have already shown that V of an isolated ECSC of PE obeys the well known formula,

$$V = A\exp\left(-\frac{B}{\Delta T^0}\right) \tag{1}$$

where A and B are constants, from which it is concluded that the lateral growth is mainly controlled by the formation of two dimensional nuclei [4–6], while the ΔT^0 dependence of the lamellar thickening growth

rate (U) has not been obtained and the molecular mechanism has not been solved at all.

Fischer *et al*. and Geil showed that the long period of the stacked lamellae (L_p) increases linearly against logarithmic time ($\log t$), from which the lamellar thickening rate (W) was estimated using the definition,

$$W = \frac{dL_p}{d\log t} \tag{2}$$

They showed that the W decreases with increase of ΔT^0 [7–9].

The purposes of this paper which we will name the Part II paper is 1) to obtain the ΔT^0 dependence of U of an ECSC, $U = C\exp(-D/\Delta T^0)$ will be shown, 2) to explain why the ΔT^0 dependence of U shows the same formula as that of lateral growth rate V, 3) to explain why U increases with increase of ΔT^0, which is just opposite to the well known fact that the lamellar thickening rate of stacked lamellae decreases with

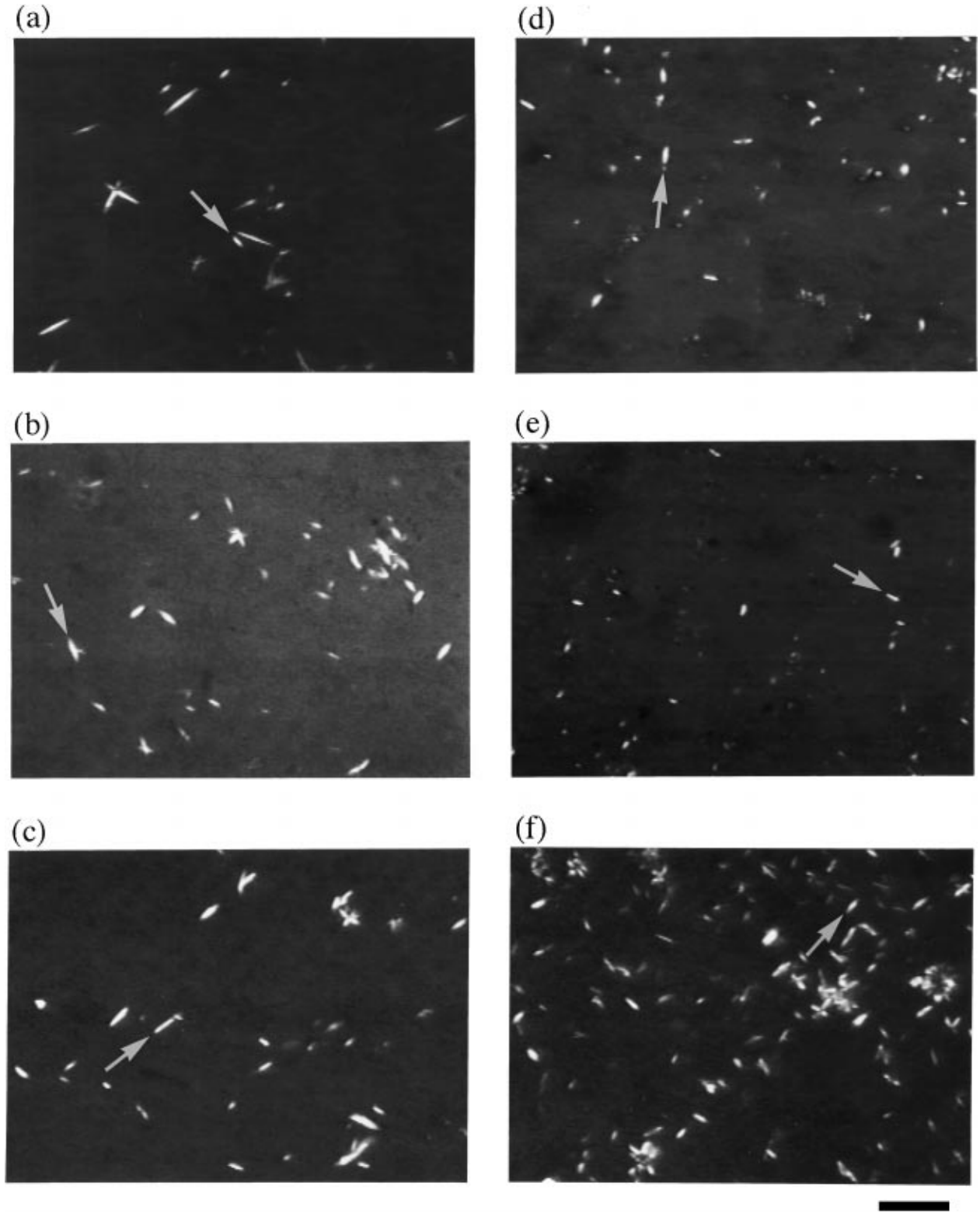

Figure 1 Polarized optical micrographs of ECSCs crystallized at $P = 0.4$ GPa. Arrows show leaf-like or cigar shapes. (a) $\Delta T^0 = 3.1$ K, (b) $\Delta T^0 = 3.6$ K, (c) $\Delta T^0 = 4.6$ K, (d) $\Delta T^0 = 6.6$ K, (e) $\Delta T^0 = 8.4$ K and (f) $\Delta T^0 = 9.4$ K. Scale bar $= 50\ \mu$m.

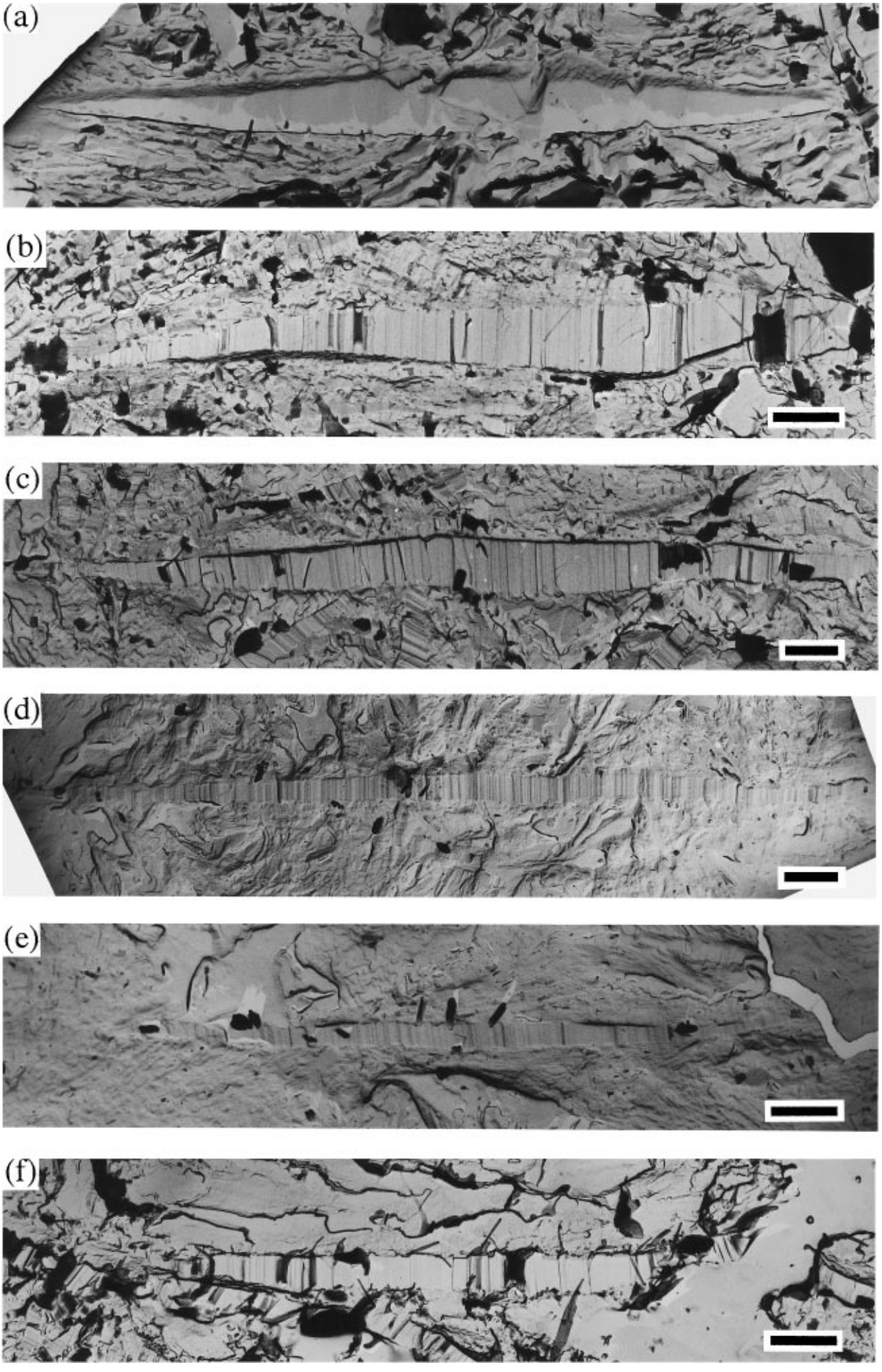

Figure 2 Transmission electron micrographs showing the linear tapered cross section of an isolated ECSC crystallized at $P = 0.4$ GPa. ECSCs shown in (a), (b), (c), (d), (e) and (f) correspond to those shown in (a), (b), (c), (d), (e) and (f) in Fig. 2. Scale bar $= 1\ \mu$m.

increase of ΔT^0, using the difference between "the primary crystallization" and the secondary crystallization and 4) to explain the origin of the tapered shape of an ECSC.

2. Experimental

Details of the materials and the experimental procedure used have been given in the previous papers [1–3]. The sample was crystallized at high pressure ($P = 0.4$ GPa) and pressure-quenched at a stage of growth where ECSCs were isolated with each other and then permanganic etched modifying Bassett's method [10] to make replicas. The replicas were observed by transmission electron microscopy (TEM: JEOL LTD., JEM-100CXII), from which the tapered shape and the lamellar thickness (l) of an isolated ECSC was observed. The lamellar thickening rate (U) were obtained from the definition, $U \equiv (1/2)(\mathrm{d}l/\mathrm{d}t)$ where t is the time. The U was obtained by applying the "mapping method" which is shown in Part I [1]. The range of equilibrium degree of supercooling (ΔT^0) in this study was 3.1–9.8 K.

3. Results

3.1. Morphology and lateral growth rate

Typical polarized optical micrographs of growing extended chain single crystals (ECSCs) crystallized at different ΔT^0s (3.1–9.8 K) are shown in Fig. 1a–f. Isolated ECSCs showed characteristic leaf like or cigar shape, the same as reported by Hikosaka and Seto at $P = 0.3$ GPa [4] or by Rastogi *et al.* at $P =$ 0.25–0.4 GPa [6]. No difference was seen in morphology in the present range of ΔT^0, which indicates that the growth mechanism does not change.

Typical transmission electron micrographs of ECSCs crystallized at different ΔT^0s are shown in Fig. 2a–f, which correspond to the ECSCs indicated by arrows in Fig. 1a–f, respectively. The linear tapered shape was confirmed on all ECSCs, from which it is concluded that the mapping method is applicable for all isolated ECSCs. In the present range of ΔT^0, little difference was observed in morphology, except that the taper angle (ϕ_{obs}) decreased with increase of ΔT^0, which will be shown in a later part of this paper.

The same ΔT^0 dependence of V as is given by Equation1, $V = A\exp(-B/\Delta T^0)$, was obtained, where $A = 3.2 \times 10^3$ nm/s and $B = 23.0$ K, which will be shown later in Fig. 6.

3.2. ΔT^0 dependence of the lamellar thickening growth rate

The lamellar thickening growth was confirmed from the linear increase of l with time t (Fig. 3). The lamellar thickening growth rate (U) was obtained from the slope of the straight lines in Fig. 3. The parameter represented in Fig. 3 indicates ΔT^0. U showed some scatter as is shown in Fig. 4 from which the standard deviation (σ) was estimated.

Fig. 5 represents the plots of $\log U$ against the inverse of ΔT^0. The error bar indicates σ. The $\log U$ vs $(\Delta T^0)^{-1}$ gives a straight line. Thus we have an experimental formula of lamellar thickening growth rate for the first time,

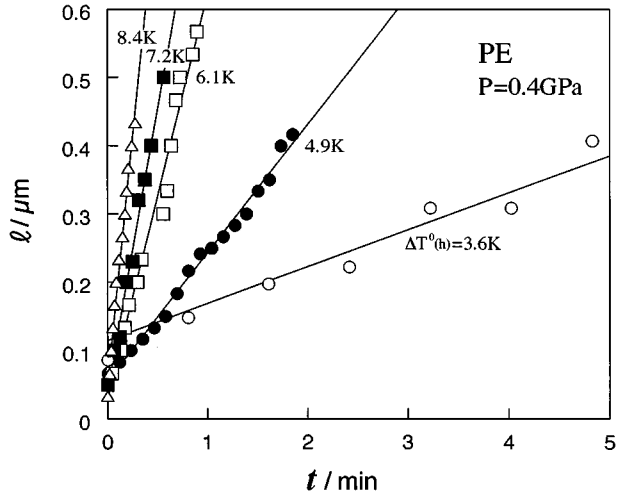

Figure 3 Lamellar thickness (ℓ) as a function of time (t) of an ECSC observed at various ΔT^0. ΔT^0(h) indicates ΔT^0 of the hexagonal crystals.

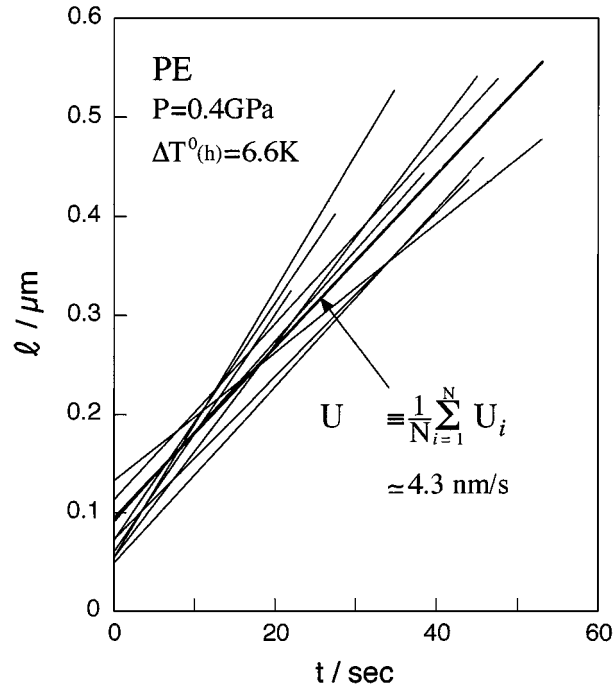

Figure 4 l against t of ECSCs showing fluctuations from which average of U and standard deviation were obtained.

$$U = C\exp\left(-\frac{D}{\Delta T^0}\right) \tag{3a}$$

where

$$C = 130 \text{ nm/s} \quad \text{and} \quad D = 20.0 \text{ K} \tag{3b}$$

It should be noted that the formula for U is the same as that for V, i.e., Equation 1. The $\log U$ is compared with $\log V$ in the same Fig. 6. This shows that $\log U$ is nearly parallel to $\log V$, which means that D is nearly equal to B, while the pre-factor C is 1/10 as large as A, that is

$$\frac{U}{V} = \frac{1}{10} \tag{4}$$

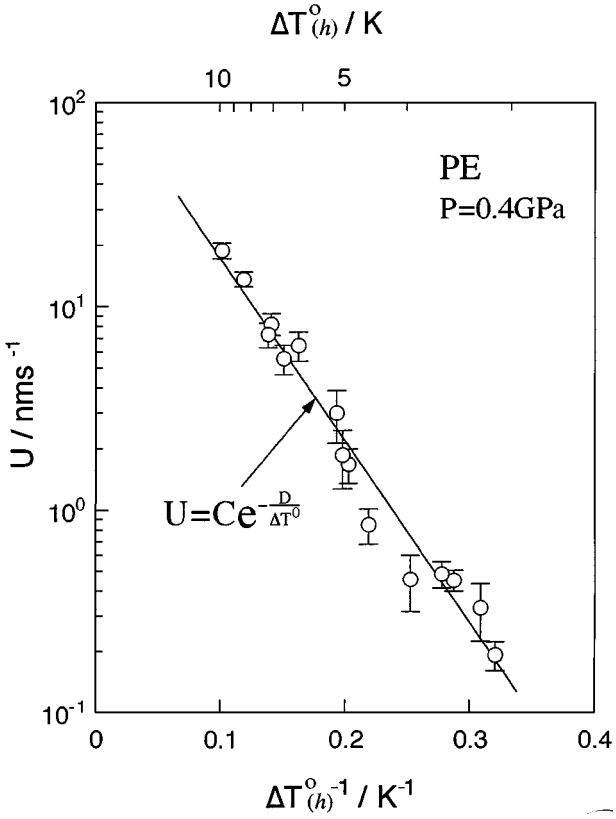

Figure 5 Logarithmic lamellar thickening growth rate (log U) of ECSCs of PE crystallized at $P = 0.4$ GPa as a function of ΔT^{0-1}. $U = C \exp(-D/\Delta T^0)$ indicates the experimental formula, $C = 1.3 \times 10^3$ nm/s and $D = 20.0$ K. Error bar shows the standard deviation (σ).

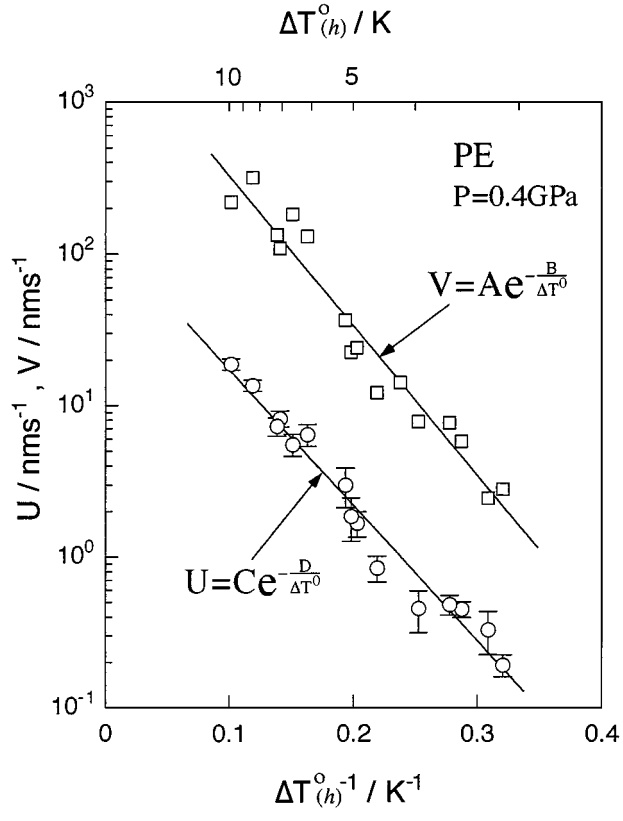

Figure 6 Comparison of log U with logarithmic lateral growth rate (log V) of ECSC crystallized at $P = 0.4$ GPa as a function of ΔT^{0-1}. The upper horizontal axis indicates ΔT^0(hex).

Thus it is concluded that both U and V show the same exponential dependence on ΔT^0. It is important to study "why do they show the same exponential dependence?" to solve the mechanism of lamellar thickening growth.

3.3. ΔT^0 dependence of the tapered shape

The tapered angle (ϕ) was observed on the cross section of an ECSC. ϕ_{obs} is plotted against ΔT^0 in Fig. 7. ϕ_{obs} gradually decreased with increase of ΔT^0. We have shown that the tapered shape is formed by coupling of the lamellar thickening growth and the conventional lateral growth [1–3]. The theoretical one ($\phi_{\text{th.}}$) given in 4.3.3 of this paper is also shown by a smooth curve in Fig. 7. $\phi_{\text{h.}}$ agreed well with the $\phi_{\text{obs.}}$, which will be discussed in 4.3.3.

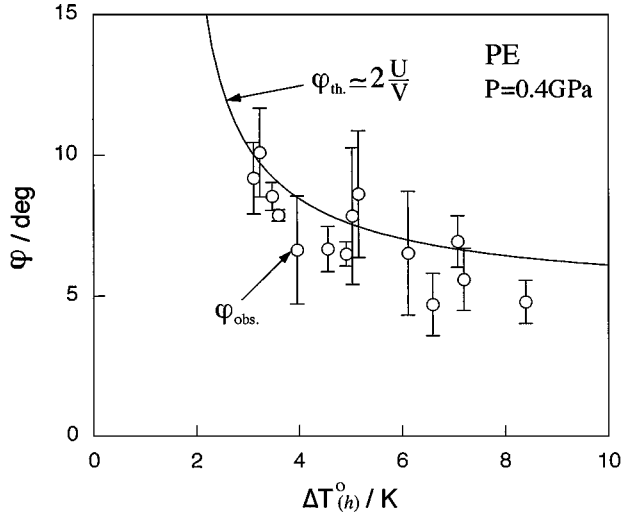

Figure 7 Observed taper angle ($\phi_{\text{obs.}}$) as a function of ΔT^0. Error bar shows the standard deviation. The smooth curve is the theoretical taper angle ($\phi_{\text{th.}}$) calculated using Equation 22 in 4.3.3 of this paper.

4. Discussion

4.1. Sliding diffusion model of the lamellar thickening growth

It is interesting that the experimental formulae of U and V given by Equations 1 and 2, respectively are essentially the same, as is shown in Fig. 6. The important question is "why do U and V show the same exponential ΔT^0 dependence?"

It is well known in the classical nucleation theory that the exponential ΔT^0 dependence of V (Equation 1) suggests that the lateral growth is mainly controlled by the nucleation process of the two dimensional nucleus on the side surface. It is well known that the nucleus can be formed only on a smooth and flat substrate on the atomic scale.

Does the same exponential ΔT^0 dependence of U also suggest that the thickening growth is controlled by two dimensional nucleation on the END surface? The answer is "No", because the end surface is a kind of "fold surface", so it cannot be flat but dynamically uneven and rough [5], as is schematically illustrated in Fig. 8. Fig. 8 shows the tapered cross section of an ECSC with uneven and rough end surface and a smooth

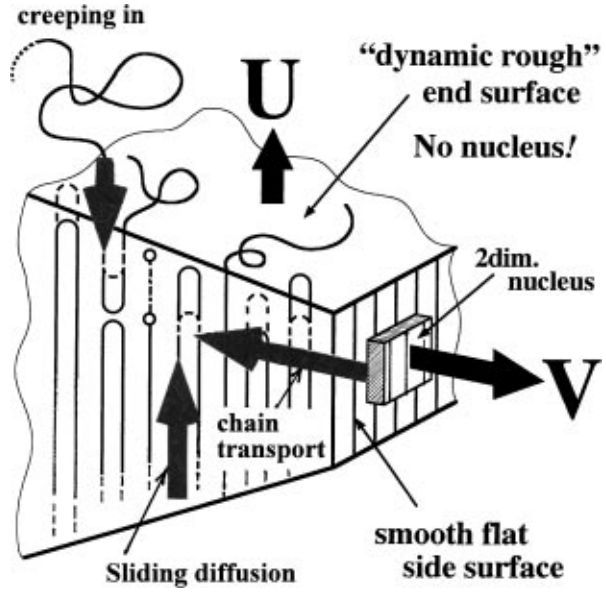

Figure 8 Sliding diffusion model of the lamellar thickening growth. Cross section of an ECSC. The end surface is dynamically uneven and rough [5], while the side surface is smooth and flat. Possible chain transportation processes by "creeping in" through the end surface and that through the nucleus on the side surface are shown. The transportation requires "sliding diffusion" within the ECSC. Note that the "end" surface is described by some authors as the "basal" surface : the use of this term is avoided here because of possible confusion in the presence of the taper.

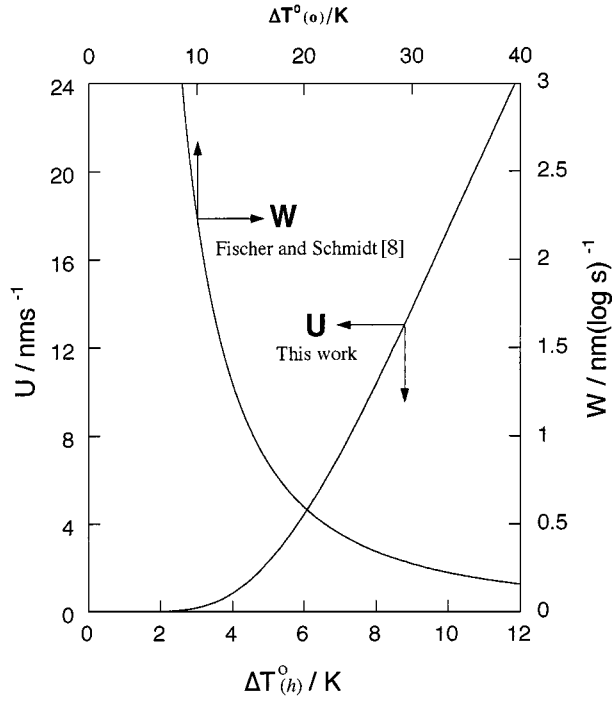

Figure 9 Positive ΔT^0 dependence of U of ECSC and negative that of the lamellar thickening rate (W) of FC crystal.

side surface on which a two dimensional nucleus is formed.

It is obvious that for the lamellar thickening growth, new chains must be transported from the melt into an ECSC. There are two possible processes of the transportation of chains, as is shown in Fig. 8. One is transportation by "creeping in" through the end surface and the other is that through the nucleus formed on the side surface. It is obvious that transported chains should be rearranged by "sliding diffusion" within the ECSC in both processes. Therefore we will propose a "sliding diffusion model of the lamellar thickening growth" where both the transportation processes are assumed to be coupled in lamellar thickening growth. The model insists that the lamellar thickening growth is controlled by both chain sliding diffusion within the ECSC and the nucleation on the side surface. The rate of the former is in proportion to $\exp(-\Delta E/kT)$ where ΔE is an activation free energy for chain sliding diffusion and kT is thermal energy and that of the latter is roughly in proportion to the lateral growth rate V. Thus we have,

$$U \propto \exp\left(-\frac{\Delta E}{kT}\right)V \tag{5}$$

This model well explains the observed fact that U and V show the same exponential ΔT^0 dependence. The other observed fact that $U/V = 1/10$ can be also well explained by the factor of $\exp(-\Delta E/kT)$. If $U = \exp(-\Delta E/kT)\ V$ is assumed, the $\Delta E = 2.3\ kT$ will be obtained for sliding diffusion within the hexagonal phase.

It is obvious that the ratio of folded chain crystals (FC crystal) is much smaller than that of extended chain crystals (EC crystal), this means that

$$\begin{aligned} \frac{U}{V} &= 1/10 \quad \text{for} \quad \text{EC crystal} \\ &\ll 1 \quad \text{for} \quad \text{FC crystal} \end{aligned} \tag{6}$$

4.2. Comparison with "lamellar thickening growth" and lamellar thickening

It should be stressed that the positive ΔT^0 dependence of U is just opposite to the well known negative ΔT^0 dependence of the lamellar thickening rate of stacked lamellae (W) in annealing or isothermal crystallization [7–9] as is schematically shown in Fig. 9. The significant contrast suggests that the mechanisms are quite different. It will be shown here that this can be explained by the difference between "the primary crystallization" of the former and "the secondary crystallization" of the latter.

4.2.1. Onset of the lamellar stacking

An isolated ECSC (= single lamella) changes into stacked lamellae after some time. The stacking is seen more frequently with increase of ΔT^0. The stacking is one of overgrowth which leads to formation of various superfine structures (textures).

Fig. 10a shows an isolated single crystal and Fig. 10b shows onset of the lamellar stacking. The onset of the lamellar stacking is considered to be related to the generation of a screw dislocation, as has been pointed out by Bassett *et al*. on FC single crystals [11]. After the onset of stacking, the number of stacked lamellae increases with time (Fig. 10c) and finally the sample is composed by fully stacked lamellae (Fig. 10d) which is commonly formed in semicrystalline polymers. (Fig. 10d is an image of a fracture surface.)

The lamellar thickening growth is defined on the isolated ECSC (Fig. 10a), while the lamellar thickening is defined on the stacked lamellae.

It should be noted that the shape of the cross section of one lamella is quite different in between the isolated lamellae and the stacked lamellae. The former shows the tapered shape (Fig. 10a), whereas the latter is flat (Fig. 10c), i.e., the lamellar thickness (l) is nearly constant within a stacked lamella. At the onset of the lamellar stacking, the l within the stacked lamellae shows a systematic change. l of the center of the lamella which is formed at first (which we will name "mother lamella") is the thickest and the l of the secondary or thirdly formed lamellae (which we will name "daughter lamella" or "granddaughter lamella") becomes thinner and thinner.

It is also to be noted that a lamella at the onset of lamellar stacking is flat at the center but tapered at its front where the lamella is not yet stacked but still isolated. This indicates that l increases rapidly with time at the front, but l changes slowly at the center, which is schematically illustrates in Fig. 11. Combination of this consideration with the observed facts on the isolated ECSC by us and on the stacked FC crystal lamellae by Fischer *et al*. [8] leads to the relations,

$$l = l^* + 2Ut \quad \text{for isolated ECSC} \tag{7}$$

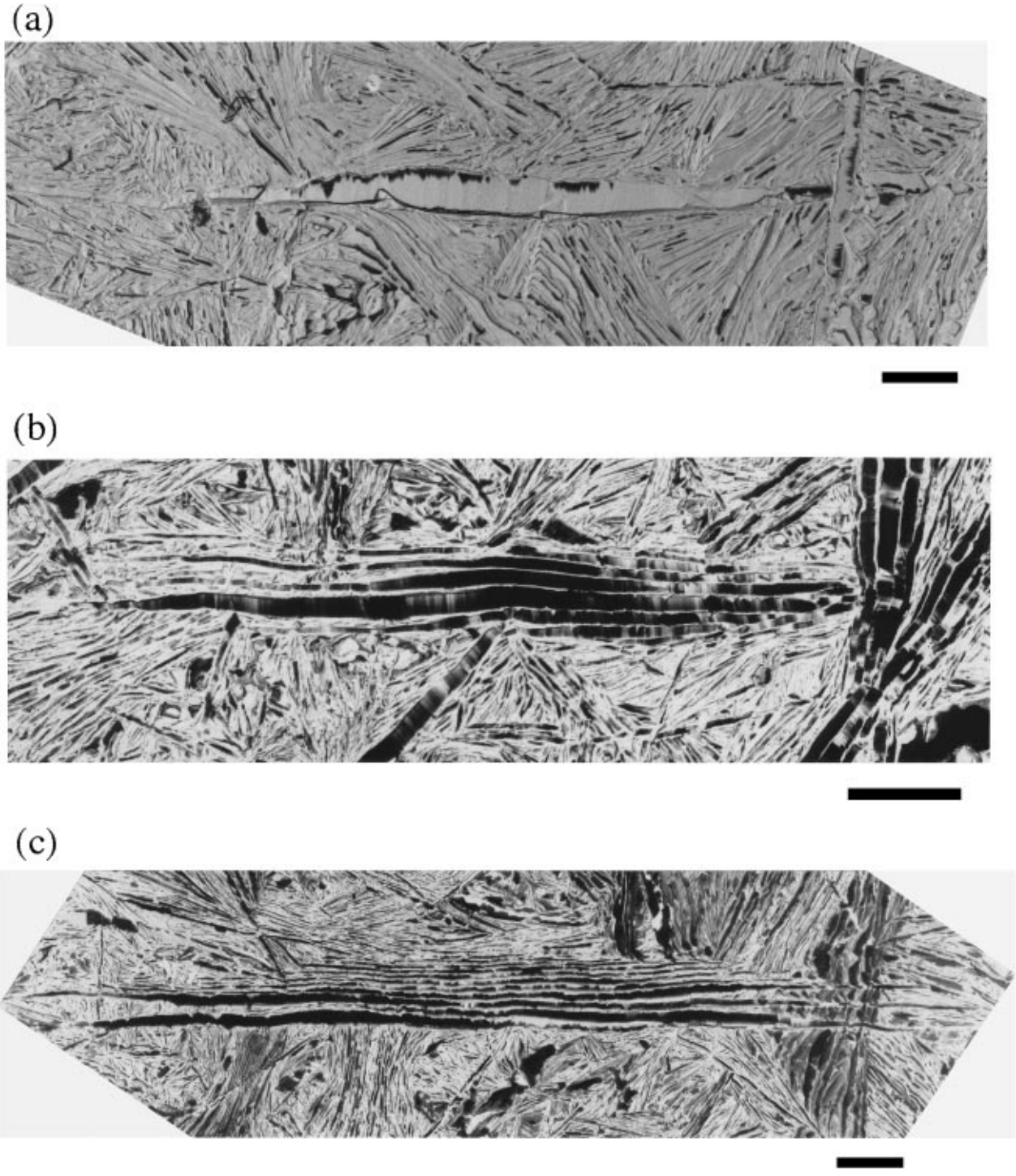

Figure 10 Transmission electron micrographs showing (a) an isolated ECSC, (b) on set of lamellar stacking and (c) stacked lamellae at $P = 0.4$ GPa and $\Delta T^0 = 6.0$ K; (d) Fully stacked and partially healed lamellae at $P = 0.5$ GPa and $\Delta T^0 = 5.4$ K. Scale bar = 5 μm. (*Continued*)

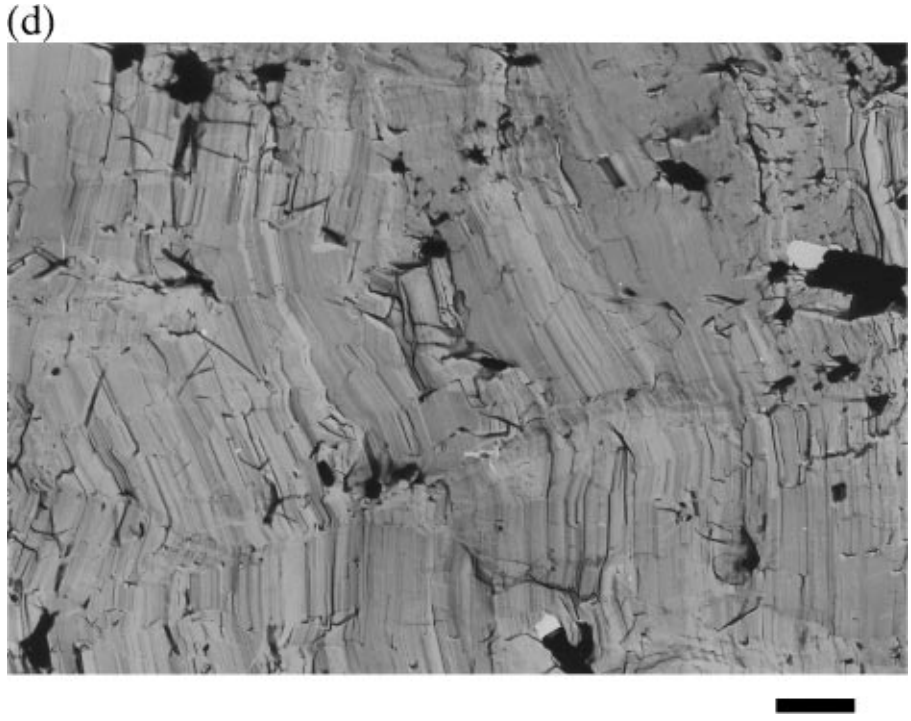

Figure 10 (*Continued*).

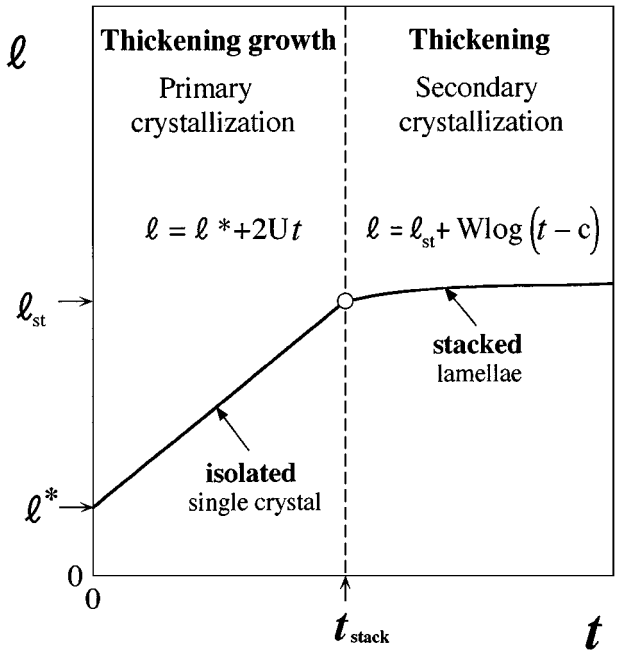

Figure 11 Linear increase of l in thickening growth and logarithmic increase of l in lamellar thickening. The former corresponds to the "primary crystallization" and the latter to the "secondary crystallization".

and

$$l = l_{\mathrm{st}} + W \log(t - c) \quad \text{for stacked lamellae} \qquad (8)$$

where $l_{\mathrm{st.}}$ is l at $t = t_{\mathrm{st.}}$, $t_{\mathrm{st.}}$ is the onset time of stacking and c is a constant.

4.2.2. Primary crystallization and secondary crystallization

In the case of thickening growth of an isolated single crystal within the melt, new chains can be sufficiently supplied through the end and side surfaces (Fig. 12a), hence it must be the primary crystallization. In the case of thickening of stacked lamellae after complete solidification, new chains cannot be supplied into an inside lamella, because there remains no melt, so lamellae have to "eat" each other by refolding [12] or chain sliding (see Fig. 12b). Therefore thickening can be regarded as a kind of "Ostwald's ripening process", hence it must be the secondary crystallization.

4.2.3. Driving force of lamellar thickening growth

The free energy of an isolated lamella (ΔG) schematically illustrated in Fig. 13 can be given by

$$\Delta G \equiv -N\Delta g + 2a^2\sigma_{\mathrm{e}} + 4al\sigma \qquad (9)$$

where N is the total number of repeating units, Δg is the free energy of fusion per one repeating unit (of an infinite crystal), a is the number of stems at the side surface, σ_{e} is the end surface free energy and σ is side surface free energy, respectively. Here the end surface corresponds to the "basal furface" of a lamellar crystal. The ΔG will decrease with increase of size of the lamella, i.e., N, which is the essential reason why lamellar thickening growth proceeds. This corresponds to decrease of relative ratio of surface area to volume of a single crystal with increase of N. Therefore the thermodynamic driving force (Δf_{iso}) for the lamellar thickening growth defined per one repeating unit can be defined by

$$\Delta f_{\mathrm{iso}} \equiv -\frac{\partial \Delta G}{\partial N} = -\frac{\Delta G}{N} = -\Delta g + \frac{2\sigma_{\mathrm{e}}}{l} + \frac{4\sigma}{a} \qquad (10)$$

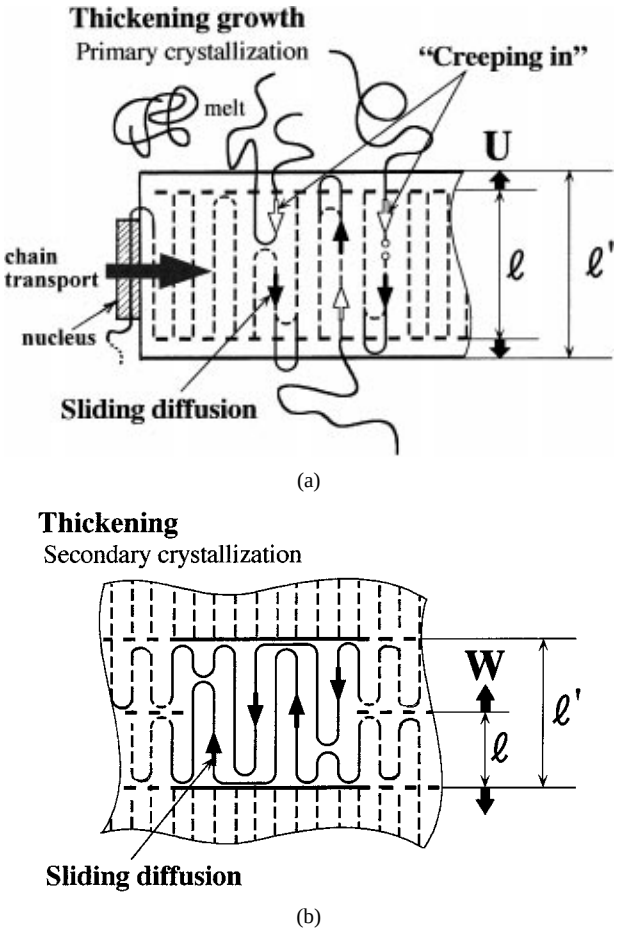

Figure 12 Schematic illustration the cross section of an isolated lamella and stacked lamellae showing the difference between (a) the "primary crystallization" and (b) the "secondary crystallization".

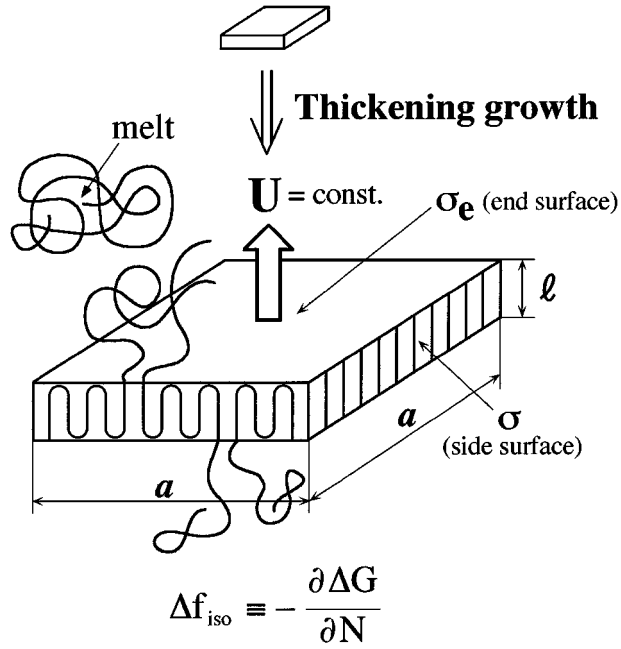

Figure 13 Lamellar thickening growth of an isolated single lamella within the melt from (a) a small one to (b) a giant one. Definition of driving force of an isolated lamella ($\Delta f_{iso.}$) is shown.

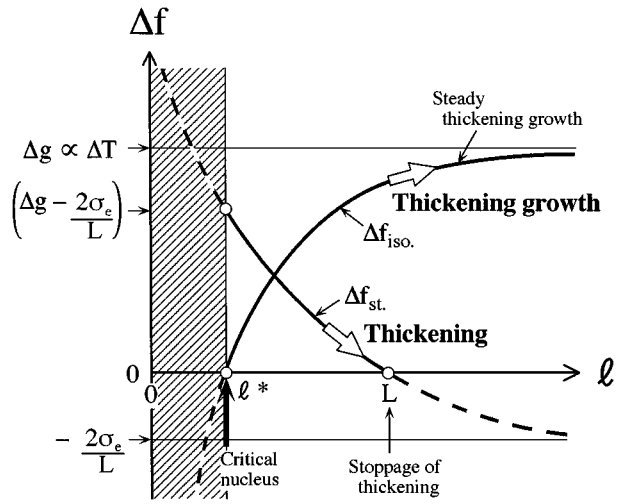

Figure 14 Driving force of an isolated lamella ($\Delta f_{iso.}$) and that of stacked lamellae ($\Delta f_{st.}$) as a function of l. $\Delta f_{iso.}$ saturates to Δg with growth, which predicts steady thickening growth, while the $\Delta f_{st.}$ approaches zero, which predicts stoppage of thickening.

where $N = a^2 l$ is used. Equation 10 predicts that Δf increases significantly with increase of l which corresponds to the early stage of thickening growth and that Δf saturates to Δg for large l (Fig. 14), i.e.,

$$\lim_{l \to \infty} \Delta f_{iso} = \Delta g \qquad (11)$$

where a is assumed to be large as compared with l. Therefore thickening growth will become steady growth, i.e., l increases linearly with time t, which well explains the observed fact of the steady linear thickening growth of an ECSC.

The constant driving force predicts that there is no final goal for lamellar thickening growth, which means that an isolated lamella will be able to thicken steadily without any limit. This is a kind of nature of "the primary crystallization". It is usual that in an actual growth process, accumulation of defects or strains will suppress the steady growth in due course and "the primary crystallization" will be switched into "the secondary crystallization" through the overgrowth mechanism.

4.2.4. Driving force of lamellar thickening

Lamellar thickening is a process of conversion from thin stacked lamellae to thick ones. Some authors describe this as "stack lamellar thickening" to emphasize the distinction from "lamellar thickening growth" as dealt with above in 4.2.2. We have chosen to retain "lamellar thickening" for the process described here. Theoretically speaking, the final goal of the lamellar thickening is conversion into a single lamella. Fig. 15 shows how the stacked lamellae (within vacuum or air, not within the melt) convert ultimately into an ideal single lamella, which is secondary crystallization and a kind of "Ostwald's ripening". In the Fig. 15, W is the rate of lamellar thickening, l is the lamellar thickness of each lamella and ξ is the number of lamellae within the stack. The free energy of all the stacked lamella ΔG of Fig. 15a is given by

$$\Delta G(\xi) = -N\Delta g + 2a^2 \xi \sigma_e + 4aL\sigma \qquad (12)$$

where L is the vertical size of the stacked crystal along chain axis which is given by $L = \xi l$. ξ decreases with

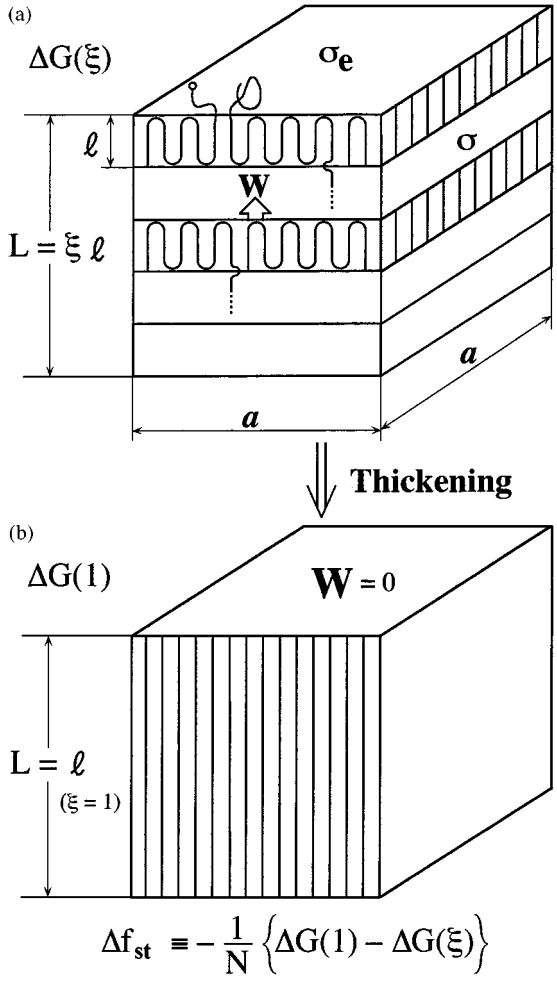

Figure 15 Lamellar thickening from (a) stacked lamellae into (b) the final stage of a single lamella. Definition of driving force of lamellar thickening ($\Delta f_{st.}$) is shown.

lamellar thickening, i.e., with increase of l. Finally ξ reaches $\xi = 1$ at the completion of lamellar thickening. So the free energy of the ideal single lamella (Fig. 15b) can be expressed as

$$\Delta G(1) = -N\Delta g + 2a^2\sigma_e + 4aL\sigma \qquad (13)$$

The driving force for lamellar thickening per repeating unit (Δf_{st}) can be defined by

$$\Delta f_{st} \equiv -\frac{\{\Delta G(1) - \Delta G(\xi)\}}{N} \qquad (14)$$

Insertion of Equations 12 and 13 into Equation 14 gives

$$\Delta f_{st}(l) = 2\sigma_e\left(\frac{1}{l} - \frac{1}{L}\right) \qquad (15)$$

where $N = a^2 l\xi$ is used. $\Delta f_{st}(l)$ is schematically illustrated as a function of l in Fig. 14. $\Delta f_{st}(l)$ is significantly large at the early stage of lamellar thickening, i.e., for thin lamellae, $\Delta f_{st}(l)$ decreases with increase of l and finally $\Delta f_{st}(l)$ reaches zero at the completion of lamellar thickening. The $\Delta f_{st}(l)$ for the initial and final stages of lamellar thickening can be obtained from Equation 15,

$$\Delta f_{st}(l) = \begin{cases} \Delta g - \dfrac{2\sigma_e}{L} & \text{for } l = l^* \text{ (initial stage, i.e., critical nucleus)} \\ 0 & \text{for } l = L \text{ (final stage)} \end{cases} \qquad (16)$$

This theoretical result well explains the well known observed fact that lamellar thickness of stacked lamellae increases linearly with logarithmic time [7–9].

4.3. Origin of the tapered shape

As is mentioned in the Introduction, the tapered shape seen on the cross section of an isolated ECSC is characteristic of a polymer single crystal and that the tapered shape is evidence for lamellar thickening growth. Here the origin of the tapered shape will be clarified.

4.3.1. Atomic or low molecular weight system does not show tapered shape

It is well known that a single crystal of atomic or low molecular weight system (such as metal or *n*-alkane) generally grows into a three dimensional shape and shows a typical crystal habit, when the growth is controlled by the two dimensional nucleation process. This means a single crystal is surrounded by flat crystallographic lattice planes and does not show any tapered shape.

Fig. 16 shows a schematic cross section of atomic or low molecular weight molecular crystal. If we assume cubic lattice for simplicity, the crystal shape is a cube (Fig. 16a) and there is no difference between the side surface and the end surface. In the case of two dimensional nucleation controlled growth, both surfaces should be smooth and flat. When a two dimensional nucleus is nucleated and sweeps on the side surface, a new layer will be formed on the side surface (Fig. 16a and b). Similarly when another two dimensional nucleus is nucleated and sweeps on the end surface, a new layer will be formed on the end surface. (Fig. 16b and c). After these steps the crystal shape will become cubic again. Further iteration will always gives a cubic shaped crystal.

4.3.2. Why does polymer show tapered shape?

Let us start from a critical primary nucleus, i.e., three dimensional nucleus (Fig. 17a). l^* and n^* are lamellar thickness and the number of stem of the critical primary nucleus, respectively. We have already shown that the lateral growth is controlled by nucleation of a two dimensional nucleus, which indicates that the side surface must be flat and smooth at the atomic or molecular scale.

In the case of the end surface, on the other hand, it must be rough on the atomic scale, irrespective of whether the crystal is orthorhombic or hexagonal. It is well known that the end surface of the orthorhombic folded chain crystal has many folds and cilia [1]. We

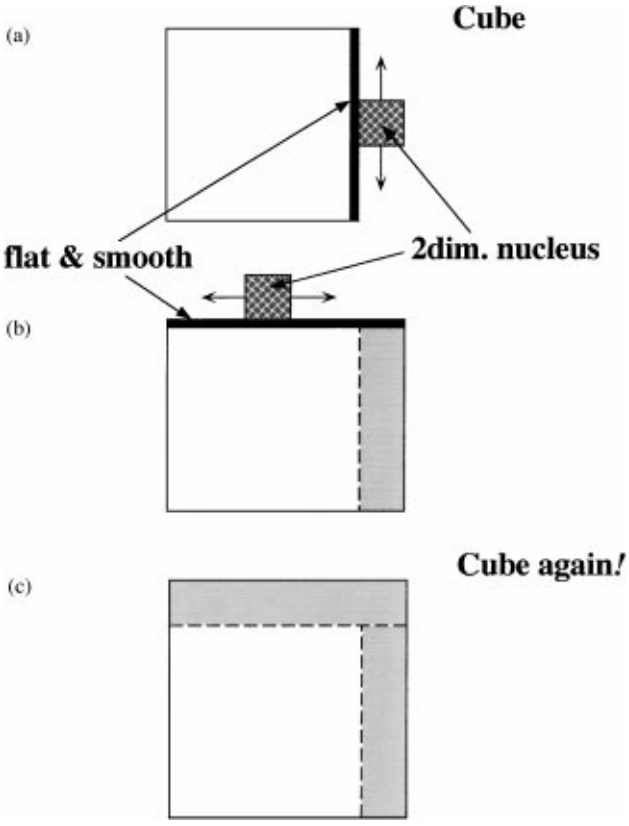

Figure 16 Growth of atomic or low molecular weight system (a and b) through surface nucleation and sweep of the nuclei; (c) The rectangular shape is always reproduced and does not change with growth.

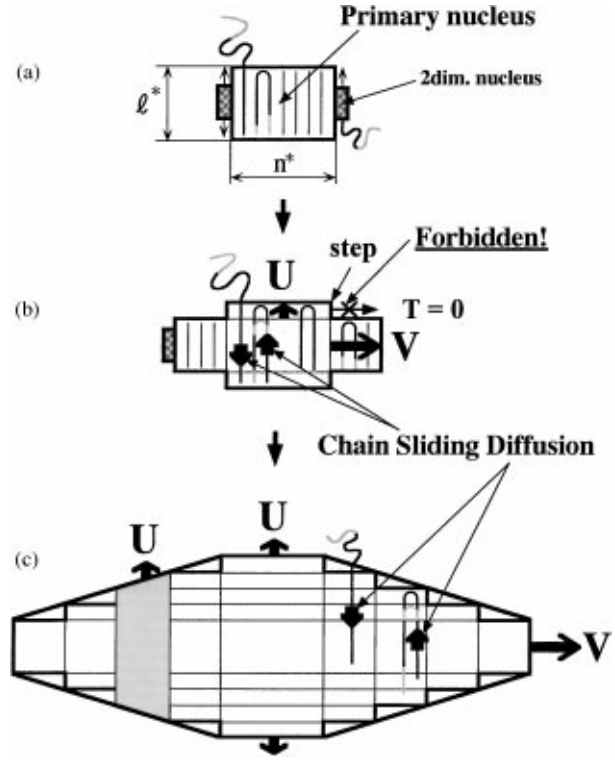

Figure 17 Origin of the "tapered shape" of polymer system. (a) Primary nucleus with rectangular shape, (b) thickening and lateral growth. The sweep of step is topologically forbidden, so the sweep rate (T) is zero and (c) iteration of (b) results in the tapered shape.

have already showed that the end surface of the hexagonal crystals of PE must be dynamically rough and uneven. We showed that the end surface free energy (σ_e) of the hexagonal crystals of PE is only 6.3×10^3 J m^{-2}, which is much less than that of orthorhombic crystals of PE. We showed theoretically that this small σ_e can be explained by the high entropy of the folded end surface which is caused by violent fluctuation of the position of the fold or cilia on the end surface. Therefore the end surface cannot be flat and smooth, so there cannot be any two dimensional nucleus on the end surface.

Fig. 17b illustrates an elementary process, forming a new end surface and side surface within some short time. On the new side surface, a new nucleus will be formed and the nucleus will sweep (= move) across the side surface and another new side surface will be formed again and again, whereas the new end surface cannot be swept by any nucleus. That is, the step A shown by an arrow in the Fig. 17b cannot sweep on the new end surface, which is an essential difference between a polymer chain system and an atomic or low molecular system. The prohibition is caused by the topological nature of the chains which forbid any nucleation on the end surface.

The new end surface only can go forward and the lamellar thickens only by chain sliding diffusion along the chain axis as has been discussed by chain sliding diffusion theory by one of the authors (M.H) [13, 14].

Therefore it is considered that the number of stem (n) increases with the lateral growth rate V by nucleation and growth of the two dimensional nucleus, while the l increases with U by chain sliding diffusion along its chain axis (see Fig. 17b). Iteration of this elementary process leads to formation of the tapered shape illustrated in Fig. 17c. Therefore it is concluded that the rough and uneven end surface caused by the topological nature of the chain system is the essential reason for formation of the tapered shape.

4.3.3. Formulation of the tapered shape

Fig. 18 shows an illustration of the cross section of a crystal. We will start from a crystal (BOA). The x and y axes and the origin O are defined in the Figure. The end and side surfaces (OB and OA, respectively) go forward with the rates U and V, respectively. The crystal thickens due to chain sliding diffusion. The V is controlled by nucleation process of the two dimensional nucleus.

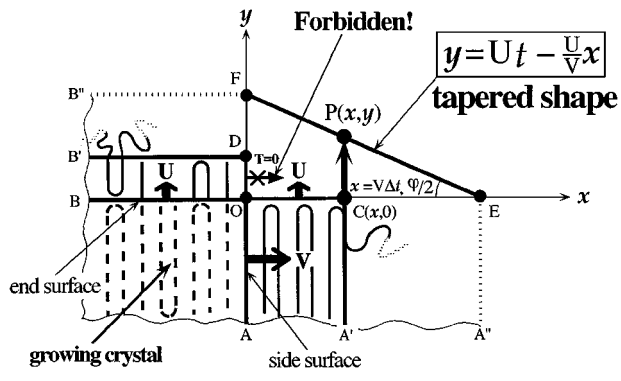

Figure 18 Formulation of the tapered shape. Trajectory of $P(x, y)$ is formulated which represents the tapered shape. See text.

Assume that after a very small (infinitesimal) time interval (Δt), the side surface OA advances to CA′ and the end surface OB advances to DB′. This means x of the point $C(x, 0)$ is given by

$$x = V\Delta t \tag{17}$$

After some time (t), they advances further to EA″ and FB″, respectively. Within Δt, new small end and side surfaces (OC and OD, respectively) are formed. In this model, the new end surface OC can thicken, while the advance of the new side surface OD is forbidden (that means the normal growth rate (denoted T) is equal to zero, i.e., $T = 0$, as is discussed in references [1, 2, 5]. So after some time t, the thickness at x will increase by y which is given by

$$y = U(t - \Delta t) \tag{18}$$

Thus the point $P(x, y)$ can be described by,

$$P(x, y) = (V\Delta t, U(t - \Delta t)) \tag{19}$$

The shape of the crystal can be formulated by the trajectory of the point $P(x, y)$. The equation of the trajectory can be given by combining Equations 17 and 18

$$y = Ut - \left(\frac{U}{V}\right)x \tag{20}$$

Equation 20 gives a straight line, passing through the points E and F, which represents the linear tapered shape of the single crystal.

Therefore we have a relation,

$$\tan\left(\frac{\phi}{2}\right) \simeq \frac{U}{V} \tag{21}$$

For the usual case ϕ is roughly equal to several or ten degrees, so the Equation 21 is approximated to

$$\phi \simeq \frac{2U}{V} \tag{22}$$

$\phi_{\text{th.}}$ calculated from Equation 22 using V and U given by Equation 1 and 3 is shown as a function of ΔT^0 in Fig. 7 which well explains the observed ΔT^0 dependence of ϕ_{obs}. Thus it is concluded that the tapered shape is determined by the ratio of U to V.

5. Conclusion

1. The experimental formula of the ΔT^0 dependence of the lamellar thickening growth rate U of an isolated extended chain single crystal of PE is obtained for the first time, $U = C\exp(-D/\Delta T^0)$, where $C = 1.3 \times 10^2$ nm/s and $D = 20.0$ K.

2. A "Sliding diffusion model of the lamellar thickening growth" is proposed: the lamellar thickening growth is controlled by both chain sliding diffusion within the ECSC and the nucleation on the side surface. The predicted relation, $U \propto \exp(-\Delta E/kT)V$, where ΔE is activation free energy for sliding diffusion, well explained the observed fact that U and lateral growth rate V show the same exponential ΔT^0 dependence.

3. The positive ΔT^0 dependence of the lamellar thickening growth rate U is opposite to negative that of lamellar thickening rate W. This difference was well explained by associating the former with "primary crystallization" and the latter with "secondary crystallization", i.e., a kind of "Ostwald's ripening process".

4. The origin of the tapered shape is well explained by coupling of lamellar thickening and lateral growths.

Acknowledgement

The authors are grateful to Prof. Ohigashi of Yamagata University for his helpful discussions. This work was partly supported by Grant-in-Aid for Scientific Research (B) No. (No. 09450364).

References

1. M. HIKOSAKA, K. AMANO, S. RASTOGI and A. KELLER, *Macromolecules* **30** (1997) 2067.
2. M. HIKOSAKA, S. RASTOGI, A. KELLER and H. KAWABATA, *J. Macromol. Sci. Phys.* **B31** (1992) 87.
3. M. HIKOSAKA, K. AMANO, S. RASTOGI and A. KELLER, "Crystallization of Polymers" (Kluwer Academic Press, London, 1993) p. 331. NATO ASI Series.
4. M. HIKOSAKA and T. SETO, *Jpn. J. Appl. Phys.* **21** (1982) L332.
5. Idem., *ibid*. **23** (1984) 956.
6. S. RASTOGI, M. HIKOSAKA, H. KAWABATA and A. KELLER, *Macromolecules* **24** (1991) 6384.
7. W. O. STATTON and P. H. GEIL, *J. Appl. Polym. Sci.* **3** (1960) 357.
8. E. W. FISCHER and G. F. SCHMIDT, *Angew. Chem.* **74** (1962) 551.
9. A. PETERLIN, *Makromol. Chem.* **74** (1964) 107.
10. R. H. OLLEY, A. M. HODGE and D. C. BASSETT, *J. Polym. Sci. Polym. Phys.* **17** (1979) 627.
11. D. C. BASSETT, R. H. OLLEY and I. A. M. AL RAHEIL, *Polymer.* **29** (1988) 1539.
12. P. DREYJUS and A. KELLER, *Polymer Letters* **8** (1970) 253.
13. M. HIKOSAKA, *Polymer* **28** (1987) 1257.
14. *Idem., ibid*. **31** (1990) 458.

Received 16 February
and accepted 2 March 2000